Evolution of the Pinatubo Volcanic Aerosol Column Above Pasadena, California Observed With a Mid-Infrared Backscatter Lidar

David M, Tratt and Robert T. Menzies

Jet Propulsion Laboratory

California Institute of Technology

4800 Oak Grove Drive

Pasadena, CA 91109

ABSTRACT

The evolution of the volcanic debris plume originating from June 1991 eruption of Mt. Pinatubo has been monitored since its genesis using a ground-based backscatter lidar facility sited at the Jet Propulsion Laboratory (JPL). Both absolute and relative pre- and post-Pinatubo backscatter observations are in accord with Mie scattering projections based on measured aerosol particle size distributions reported in the literature. The post-Pinatubo column-integrated backscatter coefficient peaked approximately 400 days after the eruption, and the observed upper boundary of the aerosol column subsided at a rate of -200 m men-].

Keywords: Aerosol backscatter, Mt. Pinatubo

introduction

The June 1991 eruption of Mt. Pinatubo resulted in one of the most severe stratospheric perturbations in modern history, and is certainly the most comprehensively instrumented and thoroughly investigated occurrence of its type, Absorption and scattering of solar radiation by the resultant debris plume is known to have significantly modified the global radiation budget, so that a knowledge of its growth and decay properties is an important factor in our understanding of the consequent global-scale climatic impact, Throughout the post-Pinatubo eruption period the Jet Propulsion Laboratory (JPL) ground-based atmospheric backscatter lidar facility has collected profiles on a regular basis above the lidar site near Pasadena, California (34°N, 118"W). As the volcanic cloud appears now to have substantially dissipated, it is timely to report on its evolutionary characteristics, as determined by analysis of the JPL long-term aerosol backscatter profile database. The dataset has historically been maintained at two wavelengths in the mid-IR: 9.25 μm and 10.6 μm [Ancellet, et al., 1988; Tratt and Menzies, 1994].

The JPL multiyear atmospheric backscatter archive

The JPL backscatter profile archive was initiated in 1984. Two coherent (heterodyne) detection pulsed CO_2 lidar systems contribute to the database: The JPL ground-based backscatter lidar [Menzies, et al., 1984] and the more recently developed JPL Airborne Backscatter Lidar

[Menzies and Tratt, 1994a]. The procedures developed to calibrate the response of these instruments have been extensively documented in the articles cited, while the algorithm formulated to extract absolute back scatter coefficients from the lidar return data remains essentially as described by Kavaya and Menzies [1985] and Tratt and Menzies [1994]. Throughout most of the time period covered by the dataset, collection of backscatter data has been carried out nominally on a weekly basis, However, since the Pinatubo event the frequency of acquisition was increased in order to better track development of the volcanic ejects plume.

Pinatubo observations

The immediate pre-Pinatubo period was characterized by generally low backscatter throughout the lower stratosphere and upper troposphere [Tratt and Menzies, 1994]. During the 1984-1990 timeframe there was an apparent order of magnitude decrease in the mean lower stratospheric backscatter at the 9.25 pm lidar wavelength (see Fig. 1). Further support for this observation may be inferred from aerosol optical depth trends measured by precision sunphotometer from Mauna Loa [Dutton, et al., 1994], and also from analysis of the SAGE (Stratospheric Aerosol and Gas Experiment) II 1.02 μm stratospheric extinction record. Using the SAGE 11 dataset, Brogniez and Lenoble [1991] have determined that by the end of 1989 (during the El Chichón decay period) the retrieved aerosol effective radius r_{eff} had declined to approximately 80% of its 1984 value, and that NO decreased by a factor of 3 during the same interval. Since within

the "Rayleigh regime" (i.e., particle size parameter $2\pi r/\lambda \ll 1$) the backscatter β_π[9.25 pm] may be regarded as approximate y proportional to r^6 [McCartney, 1976], then:

$$\frac{\beta_\pi(1989)}{\beta_\pi(1984)} = \frac{N_0(1989)}{N_0(1984)} \left[\frac{r_{eff}(1989)}{r_{eff}(1984)}\right]^6 \approx \frac{1}{3}\ (0.8)^6 \sim 0.1$$

The first unequivocal observation of enhanced stratospheric returns due to Pinatubo aerosols above the JPL lidar site was made on 11 July, 1991, almost four weeks after the actual eruption. The ensuing impact on stratospheric aerosol loading is evident upon inspection of Fig. 1, which tracks the development of prevailing atmospheric backscatter in four key altitude bands on an annual timescale. Fig. 2 contains a consolidated overview of the backscatter profile database commencing at the date of the Pinatubo eruption (June 15, 1991) and terminating after the first week of 1994. The lowest few km of the stratosphere began to fill in with consistent enhanced aerosol loading in the winter of 1992, with the peak aerosol backscatter levels being nearly 2 orders of magnitude above the pre-Pinatubo background (1989-90) levels. This is consistent with the observation by Deshler, et al. [1993] of the appearance of a fairly homogeneous aerosol layer of wide vertical extent above Laramie, Wyoming in early 1992, and the corresponding development of a bimodal size distribution with a significant large particle "growth" mode [Goodman, et al., 1994]. This display also reveals an annual periodicity in the tropospheric and lower stratospheric backscatter returns.

The spring period appears from this figure to be characterized by enhanced backscatter returns throughout the nominal tropopausal altitude band, connoting the probable increased rate of strat-trop exchange during that time frame. This phenomenon was discussed in greater detail in a recent article by the present authors [Menzies and Tratt, 1994b].

The oblique line in Fig. 2 tracks the observed upper extent of the ejects plume and represents a subsidence rate of -220 m men-l, (The implied sedimentation rate here corresponds to a mean equivalent particle radius of -0.2 pm.) Since the spring of 1992, by which time the lower stratosphere exhibited an enhanced aerosol column, the observed upper boundary of the aerosol column corresponds most closely with the upper extent of the large particle, or growth, mode of the aerosol which was observed at ER-2 flight altitudes by Goodman, et al. [1994]. The large particle mode should be the dominant contributor to the observed lidar backscatter, due to the relatively long lidar wavelength,

The integrated backscatter throughout the lower-stratosphere (tropopause to 23 km MSL) is depicted in Fig. 3. Data gaps notwithstanding, this figure indicates a well-defined I/e (e-fold) growth characteristic of about 130 days. S02 $\rightarrow H_2SO_4$ conversion was rapid during the post-eruption period [Deshler, et al., 1992], so that this characteristic time is representative primarily of particle growth by coagulation and deliquescent condensation processes [Russell,

et al., 1993]. By contrast, the strong seasonally-influenced oscillatory behavior of the integrated backscatter during the decay regime makes estimation of the e-fold depletion characteristic somewhat more conjectural, especially when we consider that there is some evidence to suggest that the eruptions of Mt. Spurr (61 "N, 152"W) between June and Sept. of 1992 may have introduced a secondary perturbation [Goodman, et al., 1994]. However, as a guide we may note that the oblique broken line overlaying this data represents an e-fold time of ~525 days, The apparent equilibrium between the growth and decay regimes is reached almost exactly 1 year after the eruption, which is comparable to the estimated time for full global dispersion of volcanically injected aerosols [Goodman, @ al., 1994].

Fig. 4 contains the pre- and post-Pinatubo geometric mean backscatter profiles, as derived from the multiyear database. Each profile has been compiled from approximately 24 months of data flanking the date of the Pinatubo eruption. It is readily apparent that the aerosol loading resulting from the Pinatubo episode engendered an approximate 40 - 50 fold increase in atmospheric backscatter within the lower stratosphere. The post-Pinatubo geometric mean profile is dominated by a broad, prominent maximum centered at approximately 17-18 km MS I., which appears to have been the altitude of maximum stability for the plume and has been reported by several other observing groups located at geographically diverse measurement sites [Chen, et al., 1992; Haner, et al., 1993; Jäger, 1994].

Mie scattering predictions

In situ measurements of the stratospheric aerosol size distribution are available for both the pre- and post-Pinatubo eras (e.g., Pueschel, et al., 1993), so that the application of Mie scattering considerations allows us to validate the data products generated using the JPL multiyear backscatter database. For this purpose, we have used the pre-Pinatubo unimodal and post-Pinatubo bimodal lognormal distributions measured in the lower-stratosphere over California by Pueschel, et al, [1993], These distributions are plotted in Fig. 5(a) and their characteristic parameters summarized in Table 1, in which the symbols define the standard lognormal distribution of volumetric particle number density with respect to particle radius, N(r):

$$\frac{dN(r)}{dr} = \frac{N_0}{r \ln\sigma_g \sqrt{2\pi}} \exp - \left[\frac{\ln r - \ln r_g}{4 \ln\sigma_g} \right]^2 \qquad (1)$$

where r is the particle radius, r_g the mode radius, σ_g^2 the lognormal variance, and NO is the total (i.e. size-independent) particle number density.

We have applied spherical particle Mie theory to the distributions represented in Fig. 5(a) to model the predicted backscatter performance of these aerosol assemblages over the C02 laser wavelength range relevant to the present study. The commonly-assumed 75% aqueous sulfuric

acid volcanic aerosol composition has been used, with appropriate complex refractive index measurements having been taken from Palmer and Williams [1975], while the Mie algorithm itself is based on the computational procedure of Bohren and 1 luff man [1983]. The resulting wavelength dependent lower-stratospheric backscatter predictions are depicted in Fig. 5(b), from which we may estimate a 40-fold increase in backscatter due to Pinatubo aerosols, in excellent agreement with Fig. 4.

Conclusion

A long-term C02 lidar atmospheric aerosol backscatter profile dataset acquired at Pasadena, California has been used to assess the evolutionary characteristics of the Mt. Pinatubo aerosol in the stratosphere. Absolute and relative backscatter observations are in substantial agreement with Mie scattering computations performed on measured aerosol particle size distributions of the volcanic plume. Equilibrium between the growth and decay phases of the plume occurred very nearly 1 year subsequent to the eruption, while subsidence of the inferred upper boundary of the aerosol cloud during the decay phase has been estimated at -220 m mon^{-1}.

Mode	N_0 (cm^{-3})	r_g (pm)	σ_g
Pre-Pinatubo	1.0	0.10	1.8
Post-Pinatubo (mode 1)	1.7	0.09	1.5
Post-Pinatubo (mode 2)	1.2	0.31	1.5

Table 1. Lognormal descriptors of pre- and post-Pinatubo lower-stratospheric aerosol assemblages above California (from Pueschel, et al., 1993).

References

Ancellet, G. M., R. T. Menzies, and D. M. Tratt, Atmospheric backscatter vertical profiles at 9.2 and 10.6 μm: a comparative study, Appl. Opt., 27, 4907-4912, 1988,

Bohren, C. F., and D. R, Huffman, in Absorption and scattering of light by small particles, John Wiley publ., New York, 1983.

Brogniez, C., and J. Lenoble, Analysis of 5-year aerosol data from the Stratospheric Aerosol and Gas Experiment II, J. Geophys. Res., 96D, 15479-15497, 1991,

Chen, H., J, R, Yu, and C. Y. She, Arrival of Pinatubo disturbances in the stratospheric aerosol layer over Fort Collins, CO, observed by a lidar at 589 nm, Appl. Phys. 11,55, 159-163, 1992.

Deshler, T., D. J, Hofmann, B. J, Johnson, and W. R, Rozier, Balloonborne measurements of the Pinatubo aerosol size distribution and volatility at Laramie, Wyoming during the summer of 1991, Geophys. Res. Lett., 19, 199-202, 1992.

Deshler, T., B. J. Johnson, and W. R. Rozier, Balloonborne measurements of pinatubo aerosol during 1991 and 1992 at 410 N: vertical profiles, size distribution, and volatility, Geophys. Res. Lett., 20, 1435-1438, 1993.

Dutton, E. G., P, Reddy, S. Ryan, and J. J. DeLuisi, Features and effects of aerosol optical depth observed at Mauna Loa, Hawaii: 1982-1992, J. Geophys. Res., 99D, 8295-8306, 1994.

Goodman, J., K. G. Snetsinger, R. F. Pueschel, G. V. Ferry, and S. Verma, Evolution of Pinatubo aerosol near 19 km altitude over western North America, Geophys. Res. Lett., 21, 1129-1132, 1994.

Haner, D. A., E. W, Sirko, and I, S, McDermid, Lidar observations of Mt. Pinatubo aerosols at Table Mountain (34° N), Topical Meeting on optical Remote Sensing of the Atmosphere, 1993 Technical Digest Series (Opt. Sot, Amer., Washington, DC), vol. 5, pp. 427-430.

Jäger, H., The stratosphere two years after the Pinatubo eruption, in Laser in Remote Sensing, eds. C. Werner and W. Waidelich (Springer- Verlag, 1994), pp. 51-54.

Kavaya, M. J., and R. T. Menzies, Lidar aerosol backscatter measurements: systematic, modeling, and calibration error considerations, Appl. Opt., 24, 3444-3453, 1985.

McCartney, E.J., Optics of the Atmosphere, John Wiley publ., New York, 1976.

Menzies, R. T., M, J. Kavaya, P. H. Flamant, and D. A. Haner, Atmospheric aerosol back scatter measurements using a tunable coherent CO_2 lidar, Appl. Opt., 23, 2510-2517, 1984.

Menzies, R. T., and D. M. Tratt, Airborne C02 coherent lidar for measurements of atmospheric aerosol and c1ouc1 back scatter, Appl. Opt., 1994a, in press,

Menzies, R. T., and D. M. Tratt, Evidence of seasonally dependent stratosphere-troposphere exchange and purging of lower stratospheric aerosol from a multi-year lidar dataset, J. Geophys. Res., 1994b, in press.

Palmer, K. F., and D. Williams, Optical constants of sulfuric acid: application to the clouds of Venus?, Appl. Opt. 14, 208-219, 1975.

Pueschel, R. F., S. A. Kinne, P. B. Russell, K. G. Snetsinger, and J. M. Livingston, Effects of the 1991 Pinatubo volcanic eruption on the physical and radiative properties of stratospheric aerosols, IRS '92: Current Problems in Atmospheric Radiation (Proceedings of the International Radiation Symposium, Tallinn, Estonia, 3-8 August 1992), S. Keevallik and O. Kärner, editors (A. Deepak, Hampton, VA, 1993), pp. 183-186.

Russell, P. B., J. M, Livingston, E. G. Dutton, R. F. Pueschel, J. A. Reagan, T. E. DeFoor, M. A. Box, D, Allen, P. Pilewskie, B. M. Herman, S. A, Kinne, and D. J. Hofmann, Pinatubo and pre-Pinatubo optical-depth spectra: Mauna Loa measurements, comparisons, inferred particle size distributions, radiative effects, and relationship to lidar data, J. Geophys. Res., 98D, 22969-22985, 1993.

Shibata, T., T. Itabe, K. Mizutani, and K. Asai, Pinatubo volcanic aerosols observed by lidar at Wakkanai, Japan, Geophys. Res. Lett., 21, 197-200, 1994,

Tratt, D. M., and R, T. Menzies, Recent climatological trends in atmospheric aerosol backscatter derived from the Jet Propulsion Laboratory multiyear backscatter profile database, Appl. Opt., 33, 424-430, 1994.

Figure Captions

Figure 1. Annual geometric mean aerosol backscatter in four altitude bands, as derived from the JPL backscatter profile archive.

Figure 2. Atmospheric backscatter time series over Pasadena since the eruption of Mt. Pinatubo. (The apparent discontinuities are an artifact resulting from interaction between the irregular acquisition intervals and the contour-fitting algorithm.)

Figure 3. Time dependence of integrated stratospheric backscatter in the post-Pinatubo timeframe. The estimated 130-day growth and 525-day decay e-fold characteristic times are represented by the broken lines.

Figure 4. Geometric mean atmospheric backscatter profiles for the pre- and post- Pinatubo regimes, compiled from the JPL multiyear backscatter profile database.

Figure 5. (a) Lower-stratospheric pre- and post-Pinatubo aerosol size distributions (based on Pueschel, et al., 1993).

(b) Predicted wavelength-dependent backscatter coefficient of the aerosol assemblages shown in part (a). Spherical 75% aqueous sulfuric acid

particles are assumed.

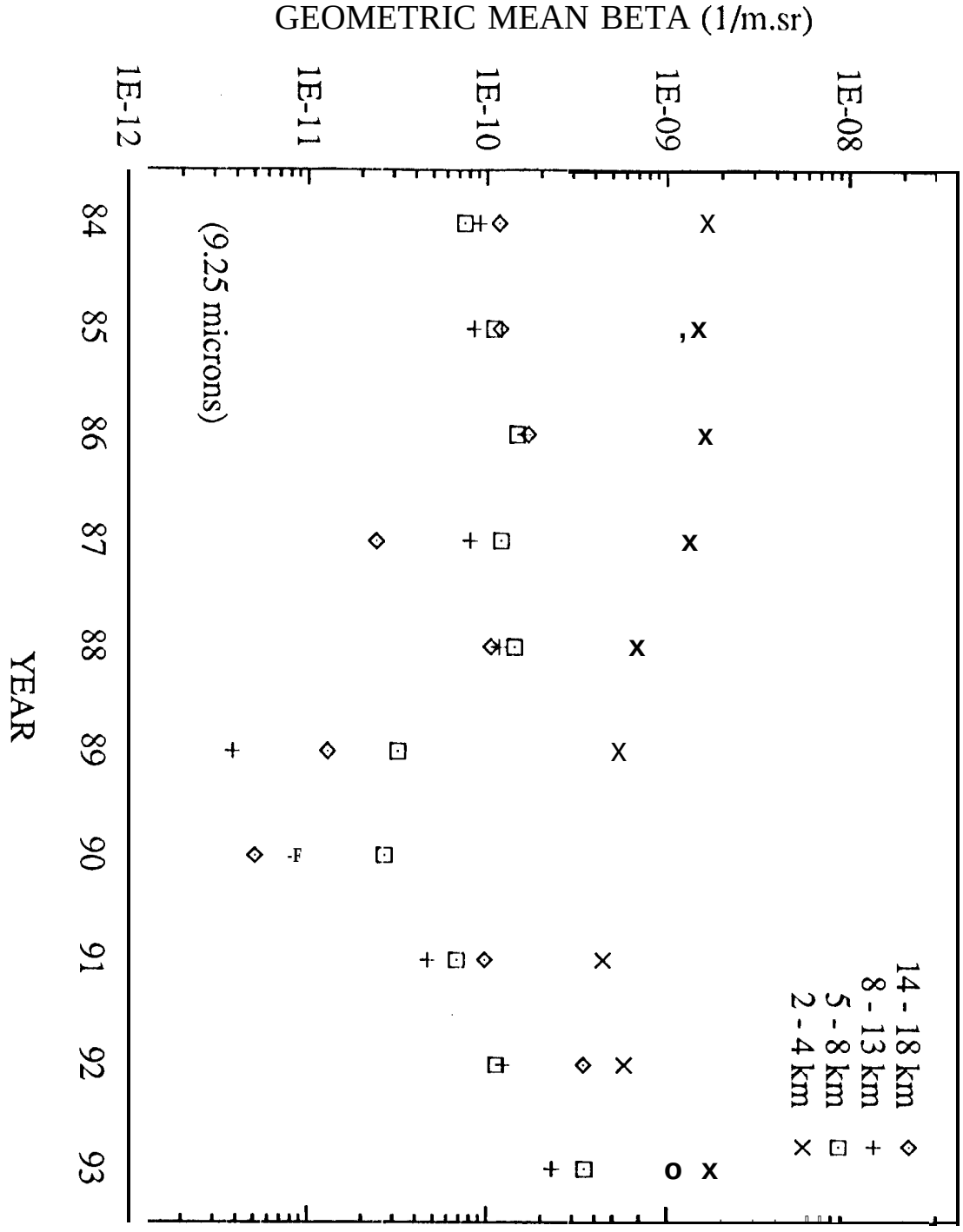
GEOMETRIC MEAN BETA (1/m.sr)
1E-08
1E-09
1E-10
1E-11
1E-12
(9.25 microns)
84
85
86
87
88
89
90
91
92
93
YEAR
14 - 18 km
8 - 13 km
5 - 8 km
2 - 4 km

Fig. 1

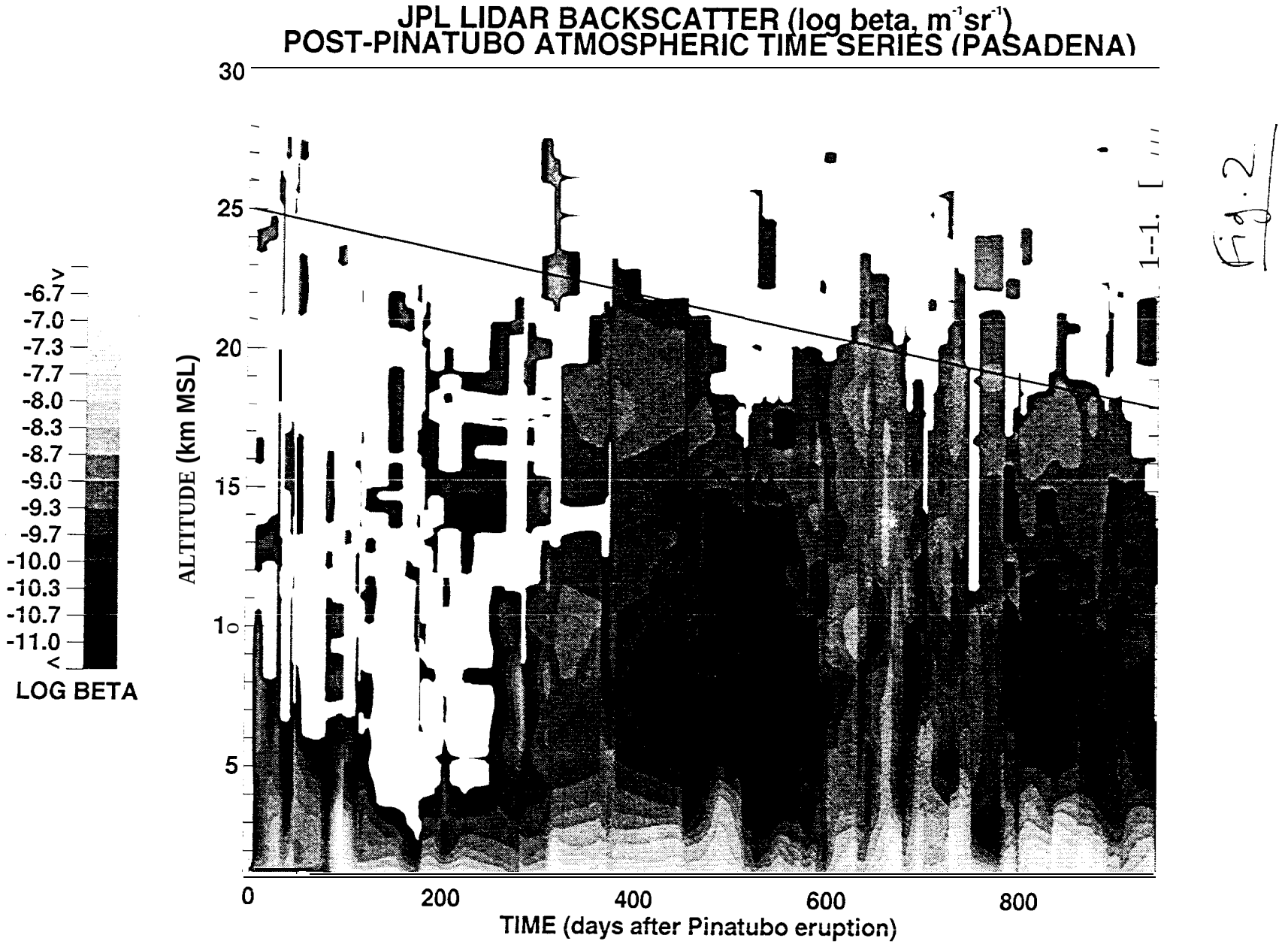
JPL LIDAR BACKSCATTER (log beta, m-1sr-1)
POST-PINATUBO ATMOSPHERIC TIME SERIES (PASADENA)
30
25
20
15
10
5
ALTITUDE (km MSL)
0
200
400
600
800
TIME (days after Pinatubo eruption)
>
-6.7
-7.0
-7.3
-7.7
-8.0
-8.3
-8.7
-9.0
-9.3
-9.7
-10.0
-10.3
-10.7
-11.0
<
LOG BETA

Fig. 2

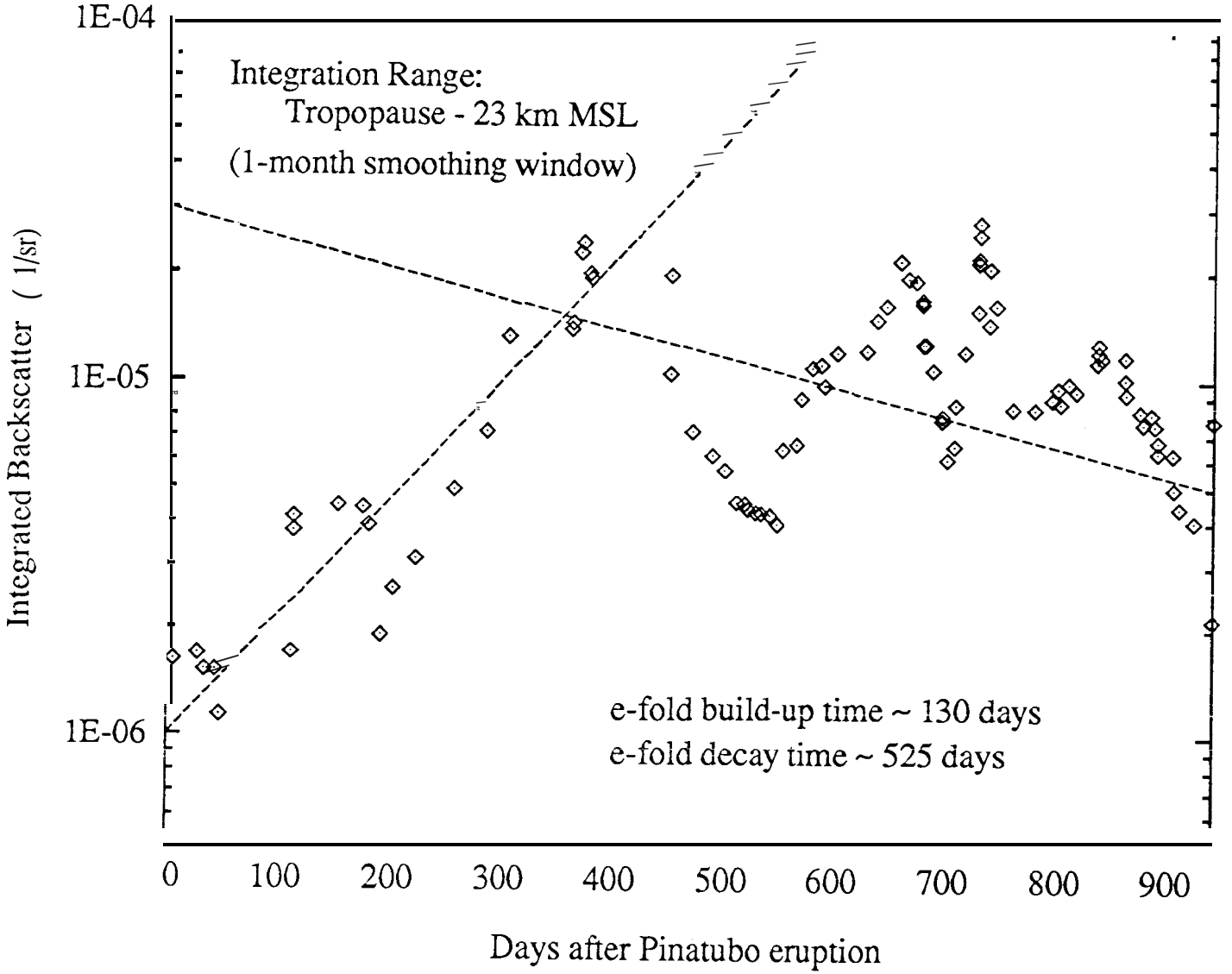
1E-04
1E-05
1E-06
Integration Range:
Tropopause - 23 km MSL
(1-month smoothing window)
e-fold build-up time ~ 130 days
e-fold decay time ~ 525 days
Integrated Backscatter (1/sr)
0
100
200
300
400
500
600
700
800
900
Days after Pinatubo eruption

Fig. 3

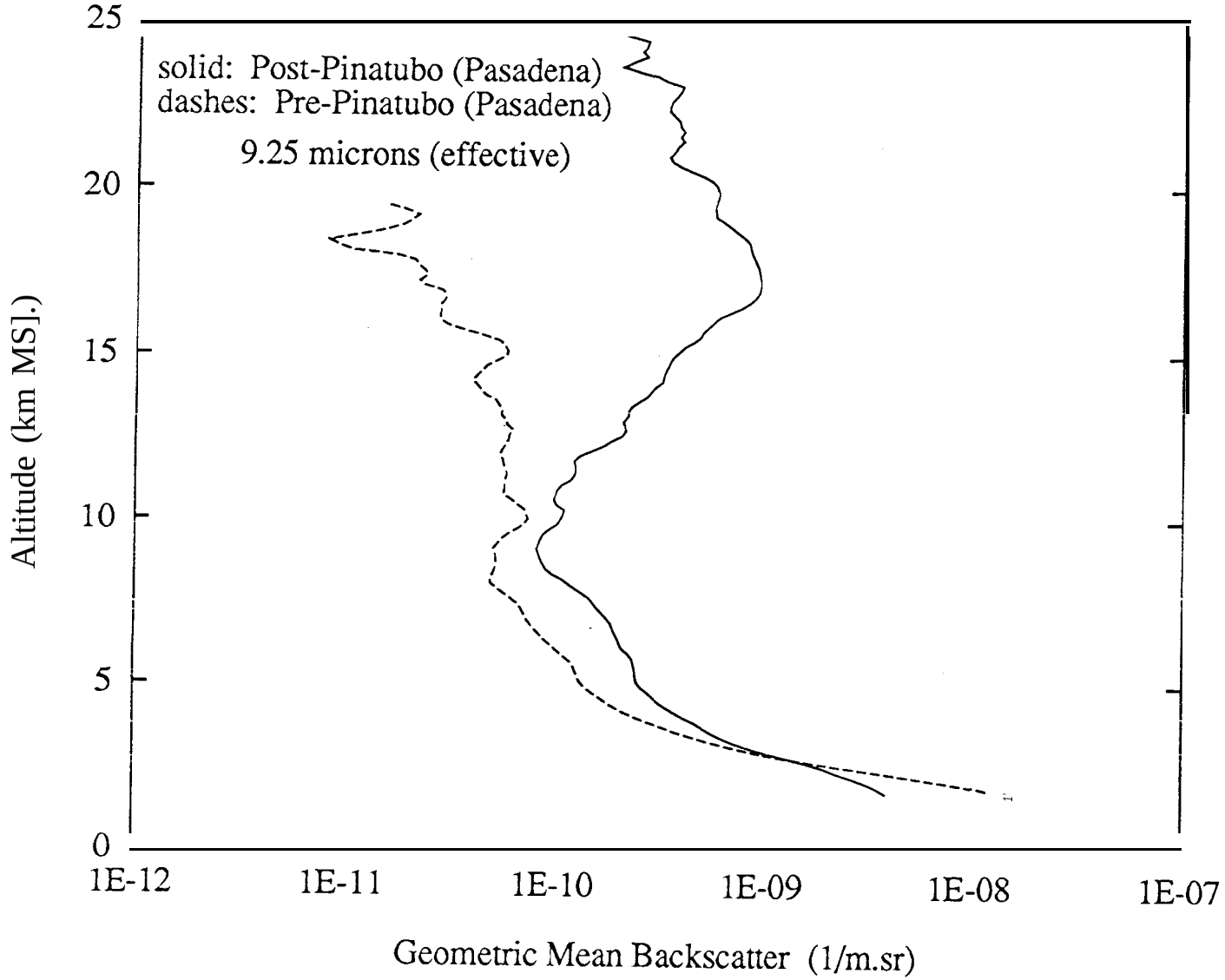
solid: Post-Pinatubo (Pasadena)
dashes: Pre-Pinatubo (Pasadena)
9.25 microns (effective)
Altitude (km MSL.)
25
20
15
10
5
0
1E-12
1E-11
1E-10
1E-09
1E-08
1E-07
Geometric Mean Backscatter (1/m.sr)

Fig. 4

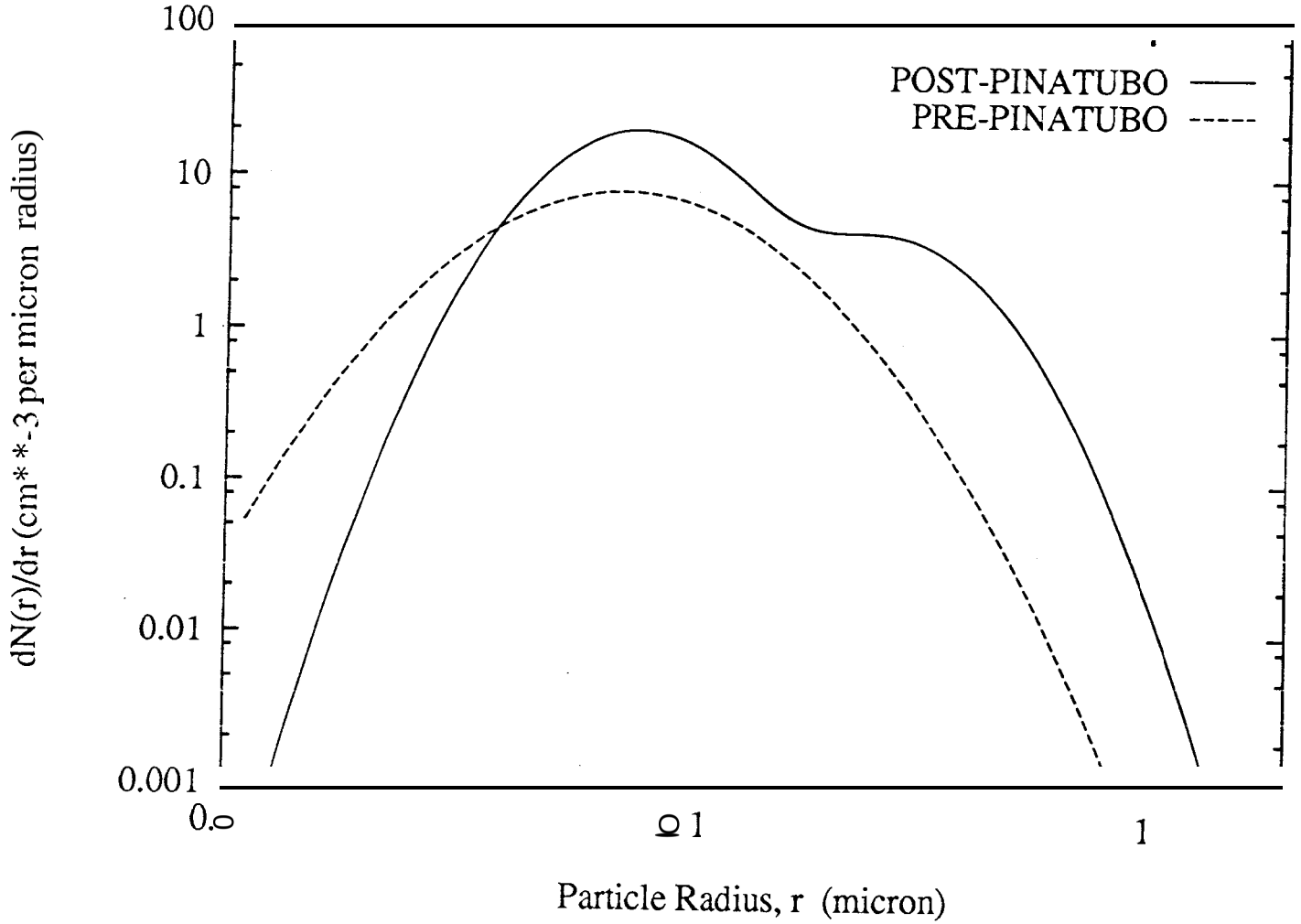
100
10
1
0.1
0.01
0.001
0.0
0.1
1
POST-PINATUBO
PRE-PINATUBO
dN(r)/dr (cm**-3 per micron radius)
Particle Radius, r (micron)

Fig. 5(a)

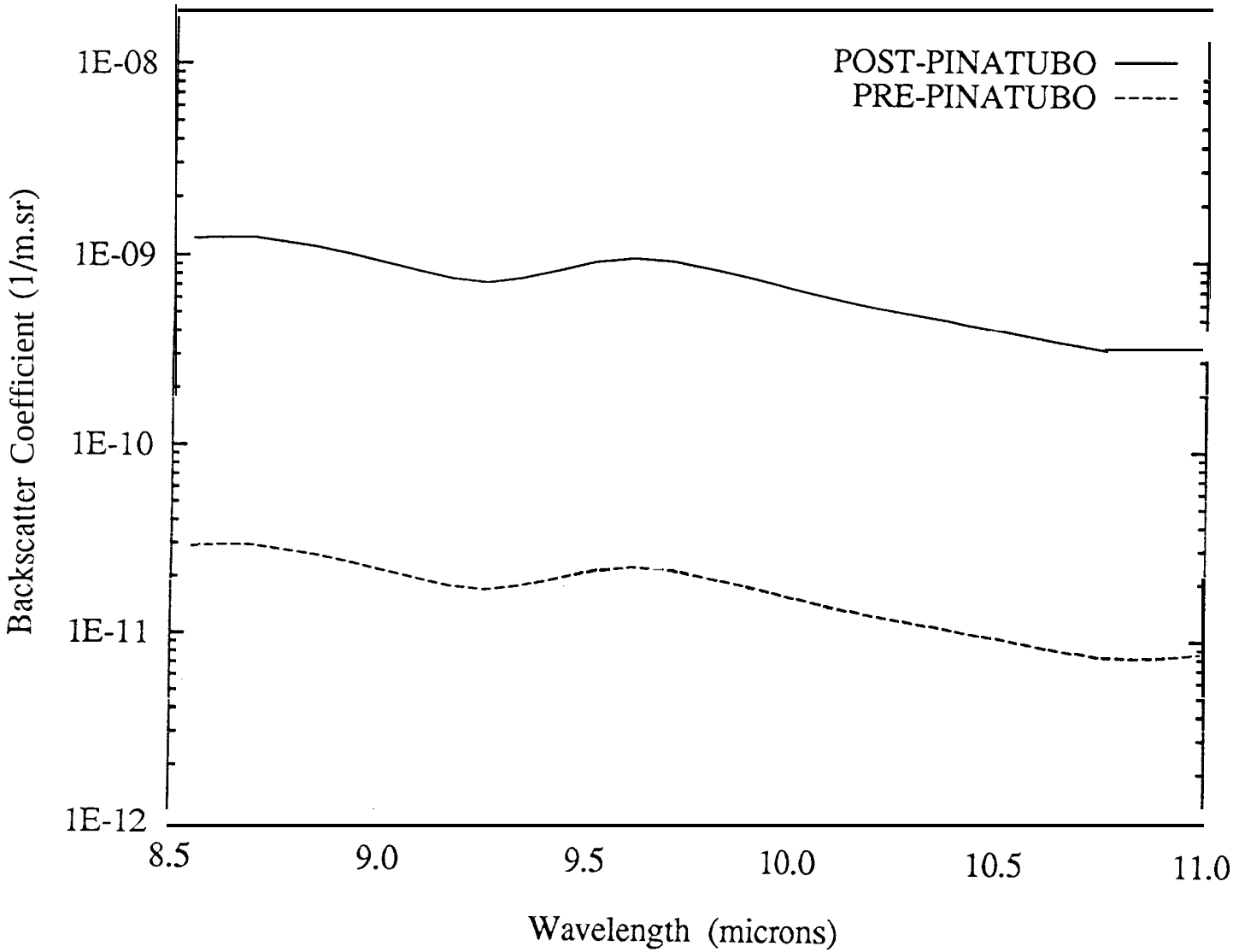
POST-PINATUBO
PRE-PINATUBO
1E-08
1E-09
1E-10
1E-11
1E-12
Backscatter Coefficient (1/m.sr)
8.5
9.0
9.5
10.0
10.5
11.0
Wavelength (microns)

Fig. 5(b)